

# Preparative liquid chromatography

## I. Influence of column efficiency on optimum injection conditions under isocratic elution

G. Crétier\*, L. Macherel and J. L. Rocca

*Laboratoire des Sciences Analytiques (UA CNRS 435), Université Claude Bernard, Lyon I, Bât. 308, 43 Boulevard du 11 Novembre 1918, 69622 Villeurbanne Cédex (France)*

(First received October 15th, 1990; revised manuscript received May 30th, 1991)

---

### ABSTRACT

Using a chromatographic simulation algorithm based on the Craig machine, CRAIGSIM, to simulate the chromatogram of a binary mixture, the optimum injection conditions corresponding to the maximum recovered amount of the solute of interest were found to depend on the column efficiency. Generally, the optimum injection concentration is an increasing function of the plate number. Consequences of this behaviour on the scale-up procedure in preparative liquid chromatography are discussed.

---

### INTRODUCTION

The goal of a preparative separation is to recover from a mixture the largest amount of one or several substances at a specified purity. A few years ago, the question was to establish whether the best injection conditions consist in concentration or volume overloading the column, *i.e.*, either using a small injection volume and increasing the injected sample concentration, or maintaining a concentration that lies in the linear part of the solute distribution isotherm and increasing the sample volume. Since then, some published results [1–4] have shown that neither of these two ways is correct: generally, both the injection concentration and the injection volume have to be increased and there are some optimum values of the two parameters for which the recovered amount of the solute of interest is maximum. The detailed study of Katti and Guiochon [2] demonstrated that optimization of injection conditions is essential when the impurity to be eliminated is the second-eluted component.

This work deals with the dependence of the optimum injection conditions on the column efficiency. This issue is of the greatest practical importance when scaling up a separation. Both the analytical and the preparative columns have to generate identical retentions, but generally they do not have the same efficiency. Hence the evolution of the optimum values of the injection parameters with the column plate number has to be known in order to extrapolate accurately the separation optimized on the analytical column to the preparative column. This paper also discusses the phenomena explaining the existence of optimum injection conditions.

This study was carried out on chromatograms simulated by means of a program based on the Craig machine using the mixed Langmuir isotherm (*i.e.*, which considers interactions between solutes during their migration). The validity of this simulation software, called CRAIGSIM, is first examined by comparing qualitatively and quantitatively some of its results with those given by the ideal model [5].

## MODEL

*Simulation of the chromatographic process*

The simulation algorithm is based on a Craig-type repetitive distribution [6]. The column is replaced with  $n_c$  stages connected in series, each stage consisting of a certain volume of mobile phase and a certain volume of stationary phase (Fig. 1). The sample is assumed to have a rectangular concentration-volume profile and is considered to fill a certain

number of mobile phase cells approaching the column inlet (Fig. 1a). The first mobile phase cell containing sample is introduced in the first stage (Fig. 1b) and after equilibration of both phases (Fig. 1c) the mobile phase is moved to the second stage, taking along its part of the sample (Fig. 1d). The process is repeated until either the sample amount in the transferred mobile phase cell becomes negligible (Fig. 1e) or the transferred mobile phase cell comes out of the column (Fig. 1f). Then the second transfer

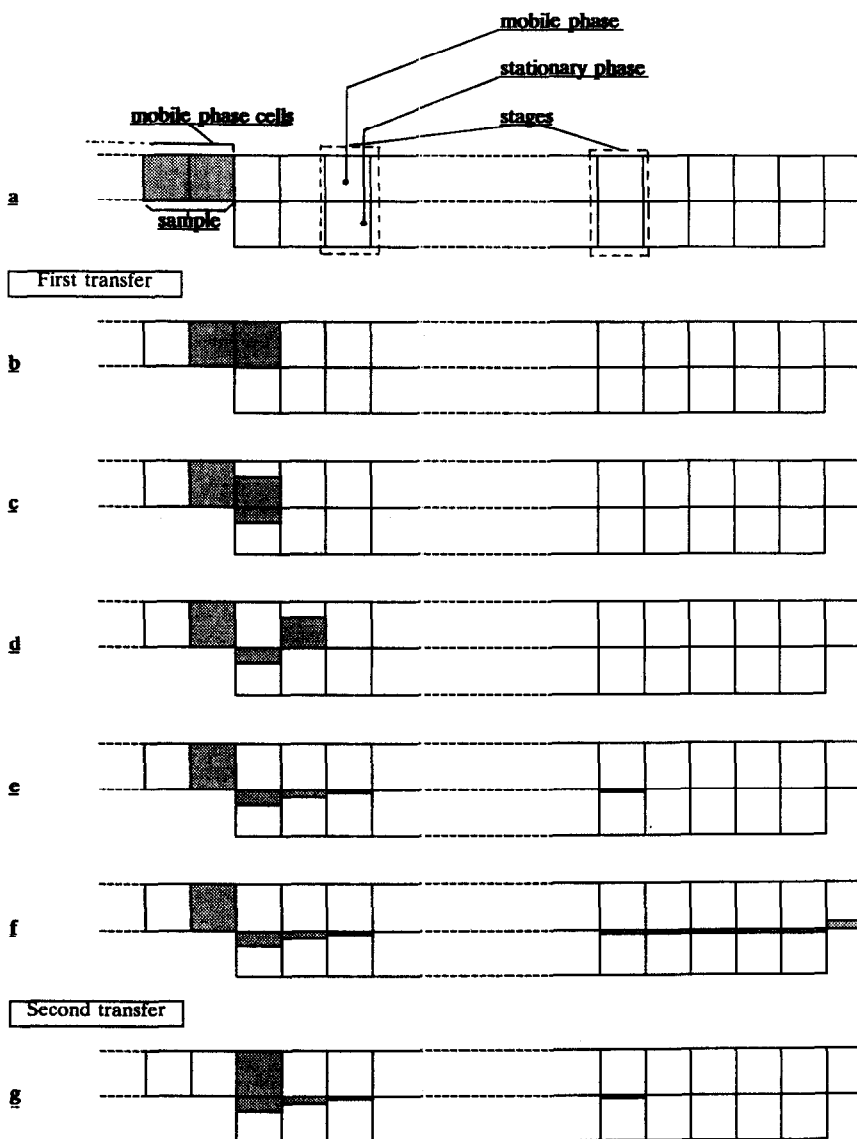


Fig. 1. Schematic diagram of the Craig machine.

is beginning: the second mobile phase cell containing the sample is placed in the first stage, and so on. Consecutive transfers flow the sample downstream. The simulated chromatogram is obtained by plotting the concentration of each solute in the mobile phase of the last stage after the last equilibration *versus* the eluted volume. The process simulates both the retention of solutes and the chromatographic dispersion. The number of theoretical plates  $N_j$  (simulated at infinite dilution for solute  $j$ ) is related to the number of stages  $n_c$  by the relationship [6]

$$N_j = (n_c + 1) \frac{1 + k'_j}{k'_j} \quad (1)$$

where  $k'_j$  represents the capacity factor of solute  $j$ . Hence a given column efficiency can be simulated by adjusting the Craig stage number.

#### *Equilibration of mobile and stationary phases in a stage*

The amount of solute  $j$  contained in the stage  $n$  at the transfer  $t$  is

$$Q_{j,n,t} = [\varepsilon C_{j,n,t}^m + (1 - \varepsilon) C_{j,n,t}^s] \frac{V_c}{n_c} \quad \begin{array}{l} j = 1 \\ j = 2 \end{array} \quad (2a) \quad (2b)$$

where  $C_{j,n,t}^m$  is the concentration of solute  $j$  in the mobile phase of stage  $n$  at transfer  $t$ ,  $C_{j,n,t}^s$  is the concentration of solute  $j$  in the stationary phase of stage  $n$  at transfer  $t$ ,  $V_c$  is the volume of the empty column and  $\varepsilon$  is the total porosity of the chromatographic bed.  $C_{j,n,t}^m$  and  $C_{j,n,t}^s$  with  $j = 1$  and  $j = 2$  are the four unknowns because, considering the process development,  $Q_{j,n,t}$  can be calculated by

$$Q_{j,n,t} = [\varepsilon C_{j,n-1,t}^m + (1 - \varepsilon) C_{j,n,t-1}^s] \frac{V_c}{n_c} \quad \begin{array}{l} j = 1 \\ j = 2 \end{array} \quad (3a) \quad (3b)$$

where  $C_{j,n-1,t}^m$  is the concentration of solute  $j$  in mobile phase of stage  $n-1$  at transfer  $t$  and  $C_{j,n,t-1}^s$  is the concentration of solute  $j$  in stationary phase of stage  $n$  at transfer  $t-1$ .

Mixed Langmuir isotherms are used to describe the solute distribution between the two phases and the interactions between the co-eluting solutes under overload conditions. The distribution of solutes 1 and 2 between the stationary and mobile phases in stage  $n$  at transfer  $t$  is represented by isotherm equations:

$$C_{1,n,t}^s = \frac{a_1 C_{1,n,t}^m}{1 + b_1 C_{1,n,t}^m + b_2 C_{2,n,t}^m} \quad (4a)$$

$$C_{2,n,t}^s = \frac{a_2 C_{2,n,t}^m}{1 + b_2 C_{2,n,t}^m + b_1 C_{1,n,t}^m} \quad (4b)$$

where  $a_j$  ( $j = 1$  or  $2$ ) is related to the capacity factor  $k'_j$  of solute  $j$  according to

$$k'_j = a_j \left( \frac{1 - \varepsilon}{\varepsilon} \right) \quad (5)$$

and  $b_j$  ( $j = 1$  or  $2$ ) is the non-linear coefficient of solute  $j$ .  $a_j/b_j$  ( $j = 1$  or  $2$ ) is the saturation concentration of the stationary phase for solute  $j$ , *i.e.*, the stationary phase concentration of solute  $j$  when its mobile phase concentration is very high. In our study, it is assumed not to depend on the solute ( $a_1/b_1 = a_2/b_2$ ). The corresponding solute amount taken up by the whole stationary phase of the column is called the column saturation capacity and is given by

$$w_s = (1 - \varepsilon) V_c \cdot \frac{a_j}{b_j} \quad (6)$$

The concentrations in the mobile and stationary phases for each solute 1 and 2,  $C_{1,n,t}^m$ ,  $C_{1,n,t}^s$ ,  $C_{2,n,t}^m$  and  $C_{2,n,t}^s$ , are calculated by considering the system of the four non-linear equations 2a, 2b, 4a and 4b; the resolution method is described in the Appendix.

## EXPERIMENTAL

### *Computer*

Chromatograms were simulated on a PC-AT compatible computer, type NX 386-25 (at 25 MHz) supplied by Unisys (Paris, France) and equipped with a Model 80387 arithmetic coprocessor. The simulation program was written in TURBO-BASIC from Borland (Scotts Valley, CA, USA).

### *Simulated conditions*

The column simulated was 15 cm  $\times$  0.5 cm I.D. with a total porosity  $\varepsilon$  of 0.8. Consequently, the column dead volume was 2.4 ml. The column plate number was varied from 150 to 900 by changing the stage number  $n_c$  from 100 to 600. We simulated the behaviour of two sample mixtures, A and B, of two solutes, 1 and 2. For each binary mixture, Table I gives the coefficients of the solute isotherms  $a_j$  and  $b_j$ , the solute capacity factors  $k'_j$ , the solute relative

TABLE I  
CHARACTERISTICS OF THE BINARY MIXTURES CONSIDERED

Mixture	Solute	$a_j$	$b_j$ (l/mol)	$k'_j$	$k'_2/k'_1$	$w_s$ (mmol)
A	1	8	0.8	2	1.5	5.89
	2	12	1.2	3		
B	1	40	8.0	10	1.2	2.95
	2	48	9.6	12		

retention  $k'_2/k'_1$  and the column saturation capacity  $w_s$ .

#### Procedure

Each simulated chromatogram corresponded to a given sample load  $Q_i$  injected at a certain total concentration  $C_i$  in a certain injection volume  $V_i$  ( $Q_i = C_i V_i$ ). For each solute, the program determined the amount  $Q_{r,j}$  recovered at 99% purity and calculated the corresponding recovery ratio or yield  $r_j$ :

$$r_j = Q_{r,j}/Q_{i,j} \quad (7)$$

where  $Q_{i,j}$  is the injected amount of solute  $j$  when the injected sample load is  $Q_i$  equal to  $Q_{i,1} + Q_{i,2}$ .

## RESULTS AND DISCUSSION

### Validation of the present Craig model

Because of interferences between migrating species, peak profiles in multi-component chromatography under overload conditions bear little resemblance to the corresponding single-component peak shapes (Fig. 2). When the two solutes are present simultaneously, the more retained solute tends to push the less retained solute in front of it; this displacement effect is beneficial for the recovery of a large amount of pure solute 1: the main part of solute 1 is eluted as a narrow and concentrated band at the beginning of the chromatogram. The displacement force of solute 2 decreases as its concentration decreases, which explains the tail on the elution profile of solute 1 under the elution profile of solute 2; this latter phenomenon has an adverse effect on the recovery ratio of the more retained compound. The peak front of solute 2 is also swept along by solute 1. The end of the peak profile of solute 2 is similar to the corresponding one without interference.

Such complex peak shapes, which are the result of interfering adsorption behaviour, are qualitatively in very good agreement with numerous published data [3-5,7]. However, in order to establish the

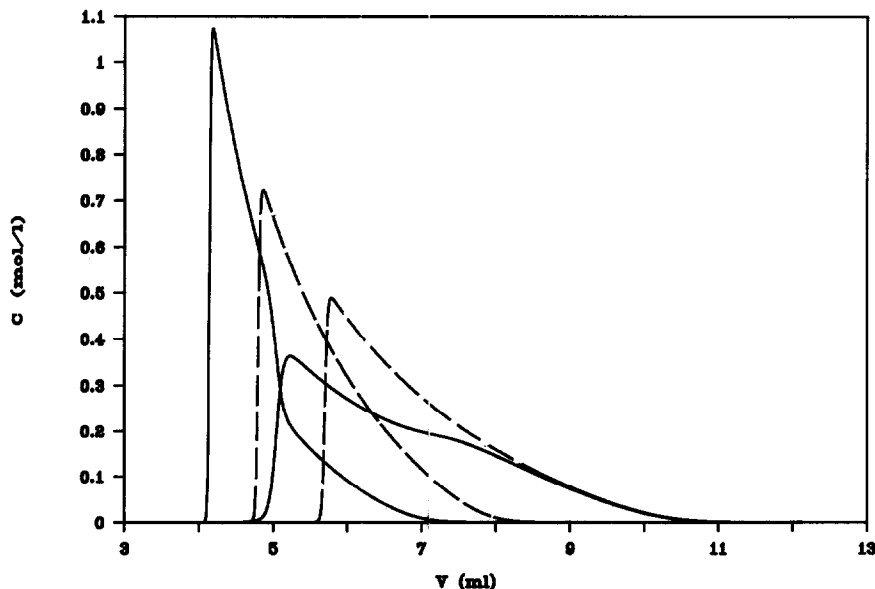


Fig. 2. Comparison of simulated chromatograms obtained by injection of (solid lines) a binary mixture and (dashed lines) the corresponding amounts of single solutes. Mixture A, relative composition 1:1.  $Q_i = 1.8 \text{ mmol} = 0.3w_s$ ;  $C_i = 2.8 \text{ mol/l}$ ;  $n_c = 400$ .

quantitative validity of our simulation program, CRAIGSIM, we need to compare some chromatograms simulated with it with the corresponding chromatograms given by the ideal model which was previously used as a reference model for describing the heavily overload separation of a binary mixture [8].

The ideal model assumes that the column efficiency is infinite, *i.e.*, the kinetics of mass transfer are so fast that there is a constant equilibrium between the two phases of the chromatographic system. The analytical solution of this ideal model in the case of a binary mixture was recently derived by Golshan-Shirazi and Guiochon [8]; each compound elution profile is composed of discontinuities and continuous parts that are described by the equations given in ref. 8. In Figs. 3–5 corresponding to the same sample amount ( $1.18 \text{ mmol} = 0.2w_s$ ) of three different mixture compositions (1:9, 1:1, 9:1) under different injection conditions, we have superimposed the chromatogram simulated by CRAIGSIM and the peak elution profiles calculated using the analytical solution of the ideal model. The agreement between the ideal chromatogram and the simulated one is very impressive; their overall shapes obviously are

very similar; further, there is quantitative agreement for the retention volumes of the discontinuities and the concentrations of the different plateaux. Of course, because of the finite column efficiency simulated by CRAIGSIM, the concentration shocks of the ideal model are slightly eroded, a small amount of band broadening appears at the peak base on each side and the band maximum does not coincide exactly. This close agreement between the two models demonstrates that CRAIGSIM software can be used to predict quantitatively elution profiles for two component separations under overload conditions.

Fig. 3 shows the elution profiles of a 9:1 mixture for a very large injected volume ( $V_i = 14.5\sigma_1$ , where  $\sigma_1$  is the standard deviation of the Gaussian peak of solute 1 observed at infinite dilution). The erosion of the top of the rectangular injection band is not complete. The profiles of the two components exhibit two plateaux. For the first peak, the second plateau corresponds to the injected concentration of solute 1 ( $0.034 \text{ mol/l}$ ) and the first plateau corresponds to a higher concentration (*ca.*  $0.087 \text{ mol/l}$ ). The more retained solute, which is the major portion of the sample, strongly displaces the less retained

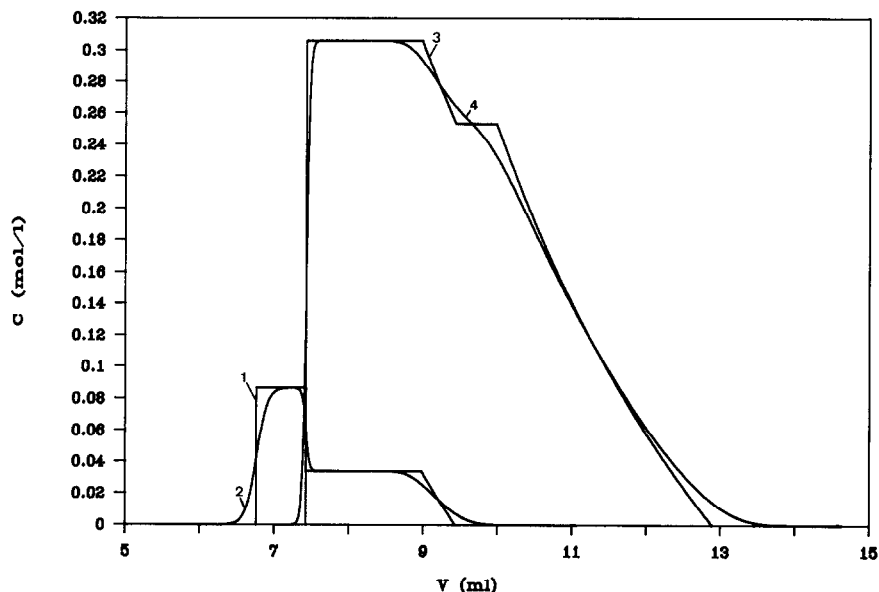


Fig. 3. Comparison between band profiles predicted by the ideal model and chromatogram simulated by CRAIGSIM for a 600-stage column. Mixture A, relative composition 1:9.  $Q_i = 1.18 \text{ mmol} = 0.2w_s$ ;  $C_i = 0.34 \text{ mol/l}$ . Curves: 1 = solute 1, ideal model; 2 = solute 1, CRAIGSIM simulation; 3 = solute 2, ideal model; 4 = solute 2, CRAIGSIM simulation.

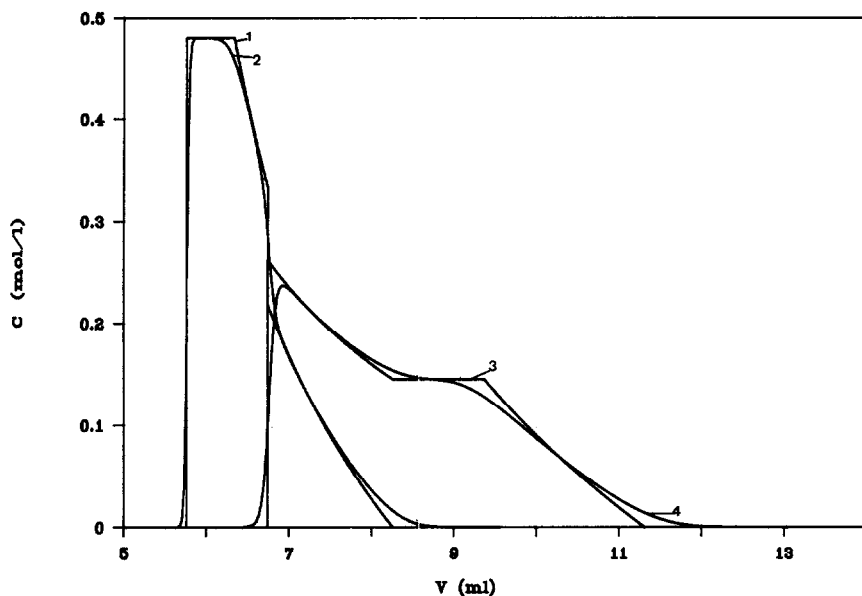


Fig. 4. Comparison between band profiles predicted by the ideal model and chromatogram simulated by CRAIGSIM for a 600-stage column. Conditions as in Fig. 3 except relative concentration of the two solutes = 1:1 and  $C_1 = 0.62$  mol/l.

solute and an excrescence, called the “displacement plateau”, appears at the front of the profile of the first component. For the second peak, the concentration of the first plateau is equal to the injected

concentration of solute 2 (0.306 mol/l) and the second plateau (which has completely disappeared owing to the chromatographic dispersion simulated by CRAIGSIM) corresponds to a lower concentra-

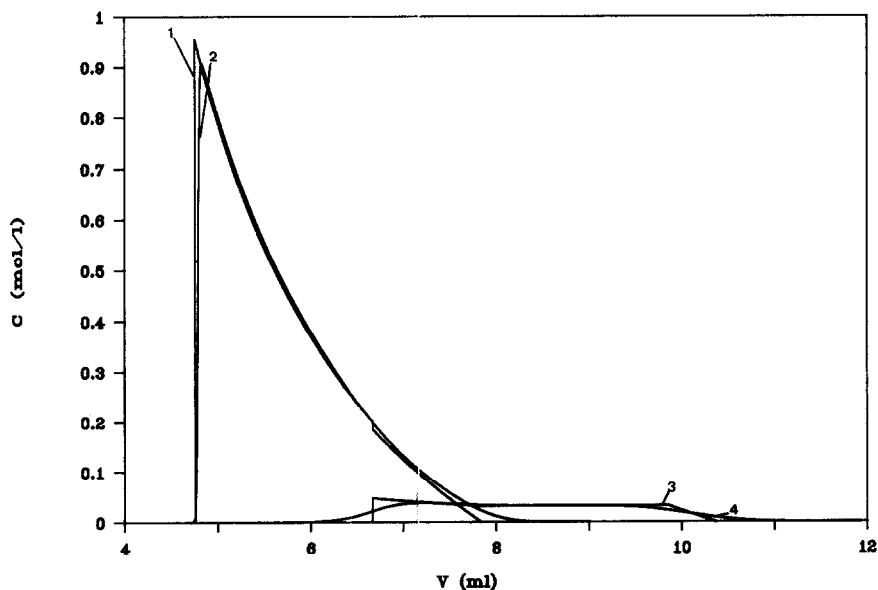


Fig. 5. Comparison between band profiles predicted by the ideal model and chromatogram simulated by CRAIGSIM for a 600-stage column. Conditions as in Fig. 3 except relative concentration of the two solutes = 9:1 and  $C_1 = 1.25$  mol/l.

tion (ca. 0.253 mol/l). The formation of the second plateau of the second peak, called the "tag-along" plateau, is due to the acceleration of the migration of solute 2 when the two solutes co-elute; the length of this plateau is increased by increasing the relative composition of the first component in the studied mixture (compare Figs. 3, 4 and 5 corresponding to 1:9, 1:1 and 9:1 mixtures, respectively).

In Fig. 5, corresponding to injection of a smaller volume ( $V_i = 0.94 \text{ ml} = 3.9\sigma_1$ ) of a 9:1 mixture, the top of the rectangular band injection is completely eroded. Because solute 2 is the minor component of the sample, the displacement effect of solute 1 by solute 2 is very weak and the plateaux of the first peak are no longer visible.

#### Design of a preparative separation

We first considered the recovered amount of purified solute as a function of both the recovery yield and the injection conditions. For a given concentration  $C_i$  of the injected mixture, the injected amount  $Q_i$ , i.e., the injected volume  $V_i$ , was gradually increased. In each run, the amount  $Q_{r,j}$  of each solute collected at 99% purity was quantified and was plotted against the corresponding recovery yield  $r_j$ . This study was carried out for mixture A at relative compositions of 9:1 (Fig. 6) and 1:9 (Fig. 7). These figures confirm the results obtained by Katti and Guiochon [2]: a recovery yield much lower than

100% is often required in order to optimize the recovered amount and the optimum recovery ratio which gives the highest recovered amount for solute 2 is always larger than that for solute 1 (from the 9:1 mixture, 65% for solute 2 instead of 40% for solute 1; from the 1:9 mixture, 97% for solute 2 instead of 50% for solute 1). These plots also show that, except at very large recovery yields, the recovered amount is affected by the sample concentration, whatever the component and the mixture composition considered.

The influence of the sample concentration and the chosen recovery yield on the recovered amount of each 99% pure solute is illustrated in detail for mixture A having relative compositions of 9:1 and 1:9 in Figs. 8 and 9, respectively. At any specified recovery yield, there is an optimum injection concentration for which the recovered amount is maximum. This optimum sample concentration is more or less critically defined. The maximum of the recovered amount is greater when the sample contains much more solute 1 than solute 2, the solute of interest is solute 1 and the acceptable recovery yield is much smaller than 100% (Fig. 8a). Hence under these conditions, the concentration of the injected mixture has to be optimized. In all other instances (Figs. 8b, 9a and 9b), the injection concentration has to be sufficient, but the use of a sample concentration much larger than the optimum does not result in

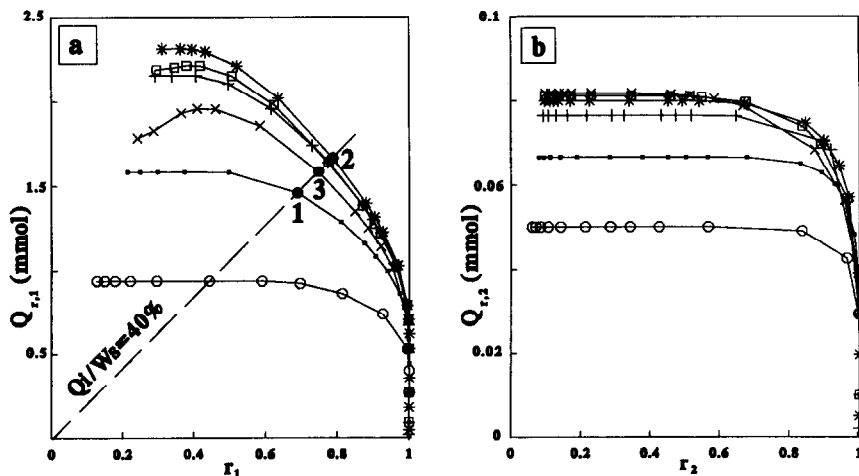


Fig. 6. Plots of the recovered amount of 99% pure solute versus the recovery yield for different injected sample concentrations. Mixture A, relative composition 9:1.  $n_c = 600$  ( $N_1 = 902$ ;  $N_2 = 801$ ). (a) Solute 1; (b) solute 2.  $C_i$ :  $\circ = 0.6$ ;  $\blacksquare = 1.7$ ;  $+$  = 5;  $*$  = 12.5;  $\square = 25$ ;  $\times = 50$  mol/l.

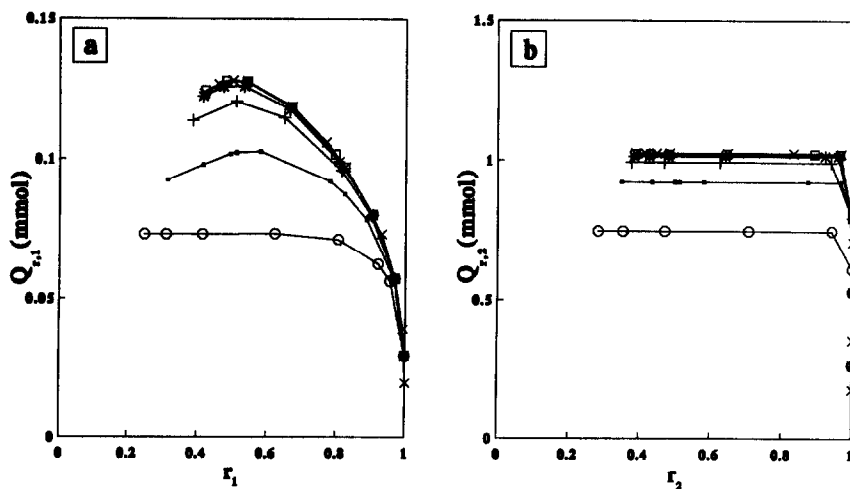


Fig. 7. Plots of the recovered amount of 99% pure solute *versus* the recovery yield for different injected sample concentrations. Conditions as in Fig. 6, except relative composition of the mixture = 1:9.

a large decrease in the recovered amount. Fig. 9b shows that the recovered amount of solute 2 from the 1:9 mixture is identical for recovery yields of 80% and 50%, whatever the injection concentration. This result was foreseeable from Fig. 7b, which demonstrates that, at any sample concentration, the recovered amount of solute 2 from the 1:9 mixture remains maximum as long as the recovery ratio is kept below 97%.

Reprocessing of an impure substance from a preceding chromatographic run is generally expensive and the optimum recovery ratio for the minimum production cost is rarely smaller than 80% [9]. Consequently, although a yield of 40% corresponds to the maximum amount of solute 1 recovered from the 9:1 mixture (Fig. 6a), it is unrealistic in practice. However, under these recovery conditions, the optimum injection concentra-

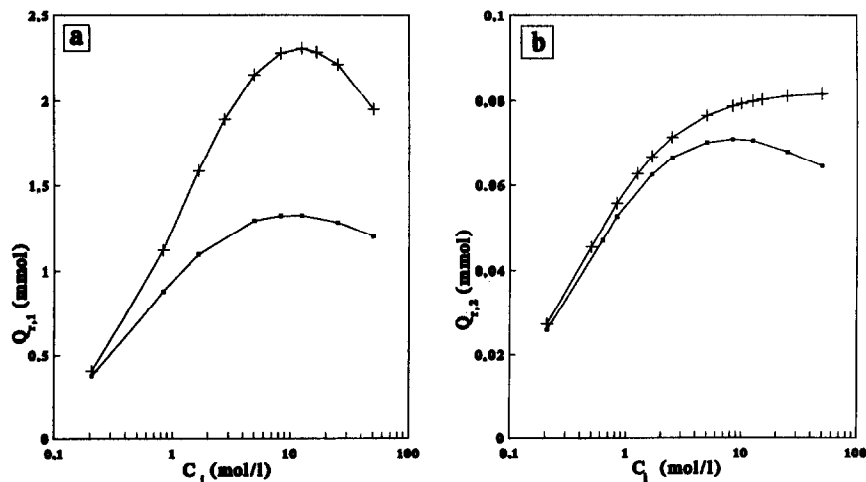


Fig. 8. Plots of the recovered amount of each 99% pure solute *versus* the sample concentration for different recovery yields. Mixture A, relative composition 9:1.  $n_c = 600$  ( $N_1 = 902$ ;  $N_2 = 801$ ). (■)  $r_j = 90\%$ ; (+)  $r_j = 40\%$ . (a) Solute 1; (b) solute 2.



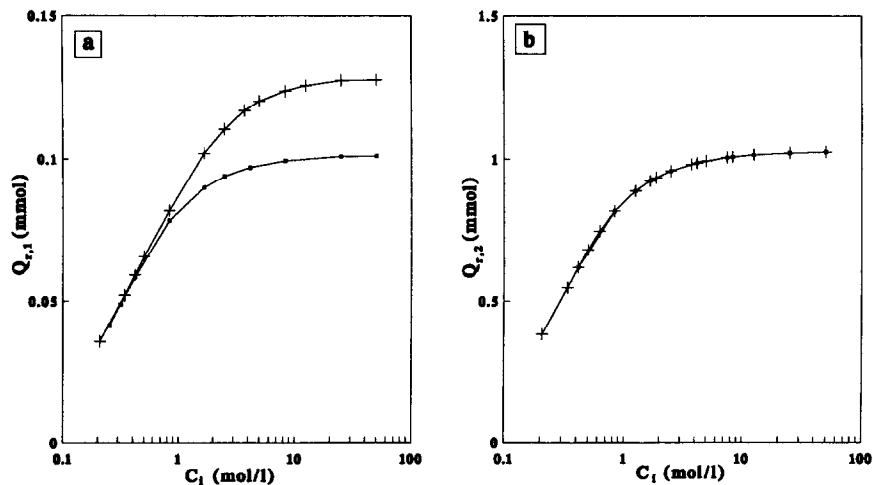


Fig. 9. Plots of the recovered amount of each 99% pure solute versus the sample concentration for different recovery yields. Mixture A, relative composition 1:9.  $n_c = 600$  ( $N_1 = 902$ ;  $N_2 = 801$ ). (■)  $r_j = 80\%$ ; (+)  $r_j = 50\%$ . (a) Solute 1; (b) solute 2.

tion is critical and, for clarity reasons, we report the results of the study of the effect of the column efficiency on the optimum injection conditions only in that case. For different column plate numbers, the variations of the recovered amount of 99% pure solute 1 from the 9:1 mixture as a function of both the sample concentration and the injection volume are plotted in Fig. 10. The recovered amount increases with increasing column plate number. The

optimum concentration corresponding to the maximum recovered amount is also an increasing function of the column efficiency (Fig. 10a). It increases from 4 to 12.5 mol/l when the stage number of the column is increased from 100 to 600 but, for an injection of 12.5 instead of 4 mol/l on the 100-stage column, the recovered amount of solute 1 decreases by no more than 12%. For 90% recovery of solute 1 from the 9:1 sample, the use on the 100-stage column

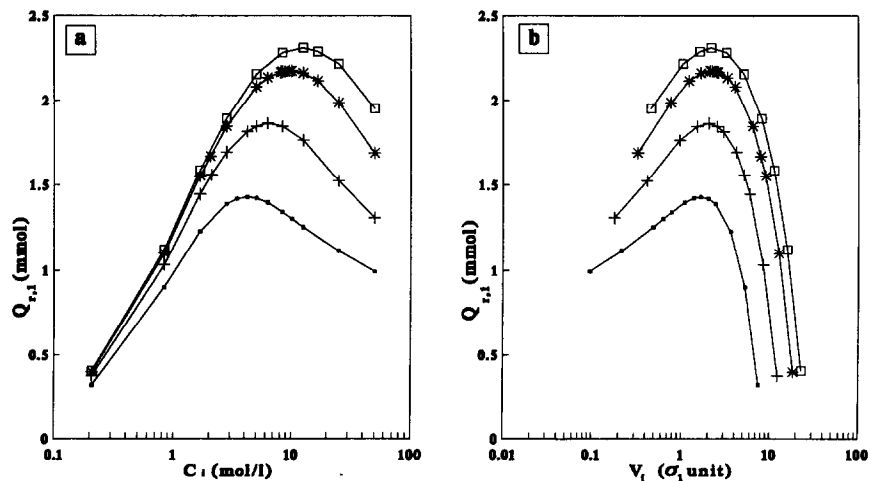


Fig. 10. Plots of the amount of solute 1 recovered at 99% purity and 40% yield versus (a) the sample concentration and (b) the injection volume for different column efficiencies. Mixture A, relative composition 9:1. (■)  $n_c = 100$  ( $N_1 = 152$ ;  $N_2 = 135$ ); (+)  $n_c = 200$  ( $N_1 = 302$ ;  $N_2 = 268$ ); (\*)  $n_c = 400$  ( $N_1 = 602$ ;  $N_2 = 535$ ); (□)  $n_c = 600$  ( $N_1 = 902$ ;  $N_2 = 801$ ).

of the same injection concentration that is optimum for the 600-stage column results in a decrease of only 4% in the recovered amount (results not shown). In other words, when scaling a separation, if necessary, the injection concentration optimized on the analytical column can be used on the preparative column, which usually contains a smaller number of theoretical plates. Then, the injection volume has to be adjusted directly on the preparative column.

Fig. 10b shows that the optimum injection volume, corresponding to the maximum recovered amount and expressed in standard deviations of the Gaussian peak observed at infinite dilution of the first solute, can be considered to be independent of the column efficiency. It varies from  $1.6\sigma_1$  to  $2.2\sigma_1$  when the column stage number ranges from 100 to 600, but a decrease of only 1.5% in the recovered

amount is incurred when the sample is injected on the 100-stage column in a volume of  $2.2\sigma_1$ . Consequently, in scale-up operation, the value of the reduced injection volume  $V_i/\sigma_1$  can first be optimized on the analytical column and then, without taking any risks, this optimum value can be adopted for the preparative column in order to adjust the injection amount.

#### *Phenomena governing the optimum injection conditions*

In order to understand the phenomena that explain the existence of the optimum injection conditions, we examined the influence of the sample concentration on the chromatogram corresponding to a given injected amount of mixture A at a relative composition of 9:1 (Fig. 11). The elution volume of

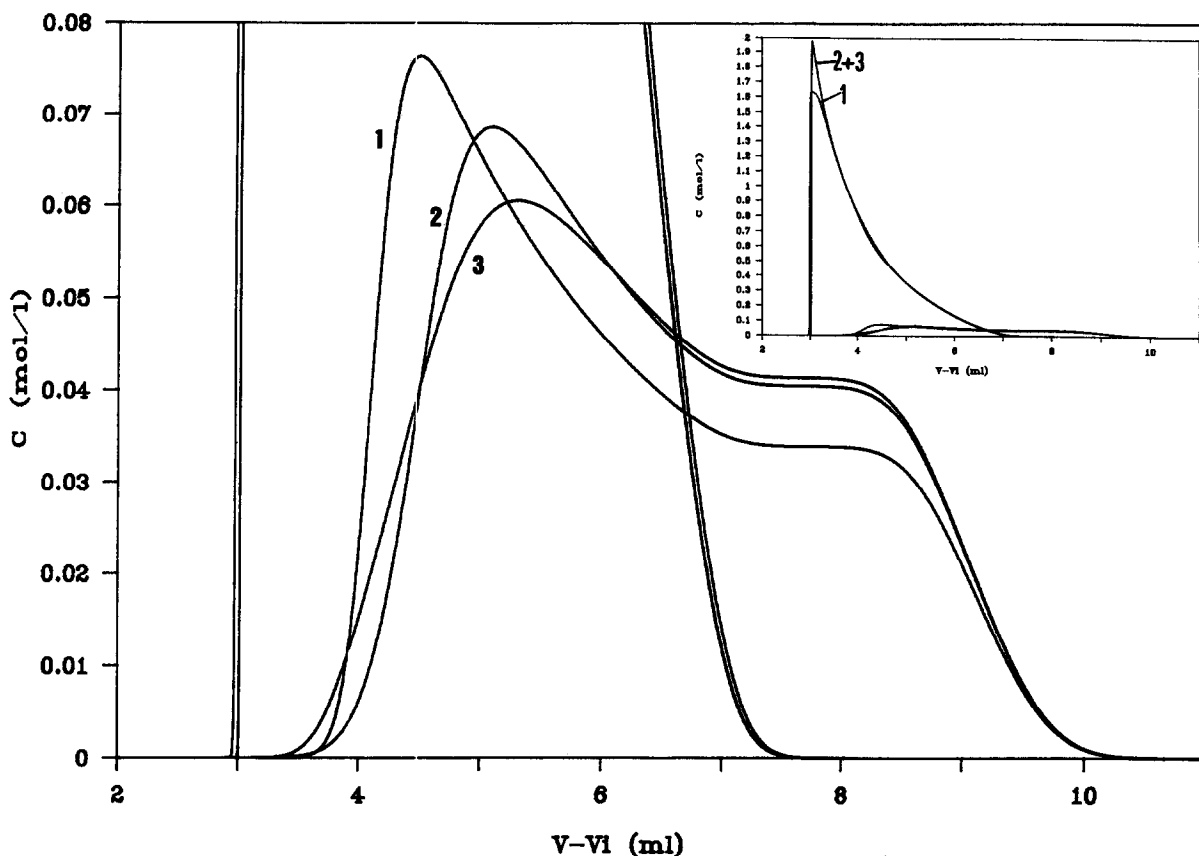


Fig. 11. Enlargement of the second peak for three chromatograms corresponding to the same injected amount,  $Q_i = 2.4 \text{ mmol} = 0.4w_s$ , of mixture A at a relative composition of 9:1 (the global chromatograms are presented in the inset).  $n_c = 600$  ( $N_1 = 902$ ;  $N_2 = 801$ ). Profile: (1)  $C_1 = 1.7 \text{ mol/l}$ ; (2)  $C_1 = 12.5 \text{ mol/l}$ ; (3)  $C_1 = 50 \text{ mol/l}$ . The elution volume is adjusted by subtracting the injection volume.

this set of chromatograms is adjusted by subtracting the injection volume. The injected sample amount is 2.4 mmol, *i.e.*, 40% of the column saturation capacity. Elution profile 2 corresponds to the optimum injection concentration for the recovery of the first-eluted solute ( $C_i = 12.5$  mol/l, data point 2 in Fig. 6a). Elution profiles 1 and 3 are obtained for a smaller injected concentration (data point 1 in Fig. 6a) and a larger concentration (data point 3 in Fig. 6a), respectively. Because the relative composition of solute 2 in the mixture is small, the tag-along effect is very strong [8]; the co-elution of the two solutes accelerates the migration of the front of the second solute and results in the formation of the plateau on the peak of solute 2. When we successively consider chromatograms 1–3, the injected concentration is increased and the injected volume is decreased because the injected amount is kept constant. The height of the tag-along plateau for the second component increases with increasing the injection concentration. Because the smaller the relative concentration of the second component the more important is the tag-along effect, the acceleration of the migration is larger for the front base of the second component, corresponding to low concentrations, than for its front top, corresponding to

larger concentrations; hence the decrease in the width of the second component with decreasing injection volume is smaller at the peak base (compare elution profiles 1 and 2). This phenomenon becomes more marked as the injected concentration is increased and finally results in band broadening at the front base of the second component, which elutes faster in the chosen representation (compare elution profiles 2 and 3). The decrease in the recovered amount of the 99% pure first component for a large injected concentration of the 9:1 mixture (data point 3 in Fig. 6a) is a consequence of this additional band broadening of the second-component front.

Fig. 12 shows that the same phenomena occur with sample mixture corresponding to a lower separation factor. It superposes the chromatograms obtained for the same load of the 9:1 mixture  $\hat{B}$ ,  $Q_i = 0.59$  mmol =  $0.2w_s$ , injected at three different concentrations,  $C_i = 0.08$ , 1.2 and 62.5 mol/l. In these experiments, the resolution at infinite dilution is equal to 1.2 instead of 1.7 for mixture A in Fig. 11. As the injection concentration is increased, the band broadening pattern seems to be qualitatively very similar to that observed for mixture A (compare Figs. 11 and 12). Quantitatively, the recovered amount of 99% pure solute 1 for the 1.2 mol/l

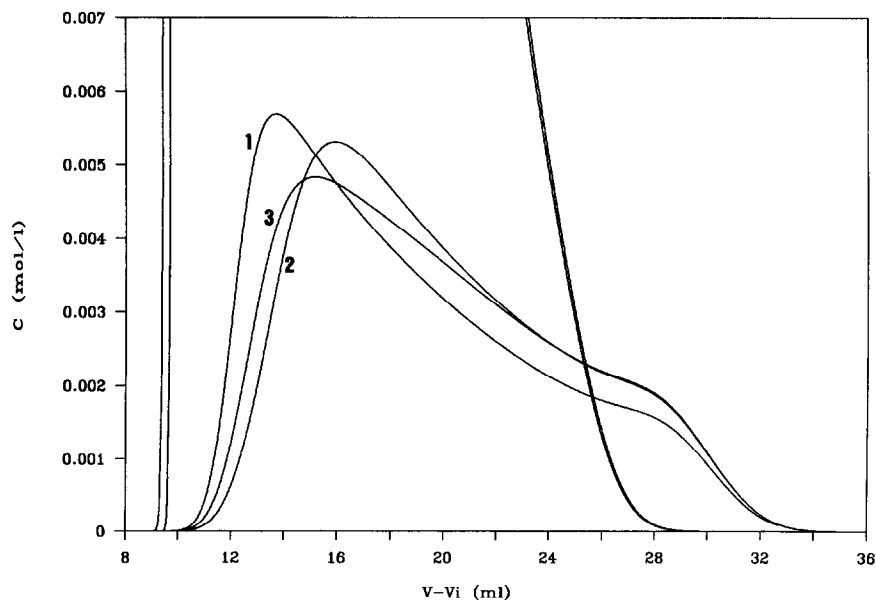


Fig. 12. Enlargement of the second peak for three chromatograms corresponding to the same injected amount,  $Q_i = 0.59$  mmol =  $0.2w_s$ , of mixture B at a relative composition of 9:1.  $n_c = 500$  ( $N_1 = 551$ ;  $N_2 = 543$ ). Profile: (1)  $C_i = 0.08$  mol/l; (2)  $C_i = 1.2$  mol/l; (3)  $C_i = 62.5$  mol/l. The elution volume is adjusted by subtracting the injection volume.

injection exceeds that for the 0.08 and 62.5 mol/l injections, namely 0.274 mmol for  $C_i = 1.2$  mol/l to 0.197 and 0.239 mmol for  $C_i = 0.08$  and 62.5 mol/l, respectively. Hence the value of 1.2 mol/l is optimum. The corresponding recovery yield of solute 1 is 51.8%.

The effect of the column efficiency on the optimum injection concentration giving the highest recovered amount is shown in Fig. 13. The sample is mixture A at the relative composition 9:1. The injected amount is kept equal to 2.4 mmol ( $0.4w_s$ ) and each curve plots, for a specified column plate number, the amount of the first solute recovered at 99% purity against the injected sample concentration. The result previously observed is found: the optimum injection concentration corresponding to the curve maximum is an increasing function of the column efficiency. It seems to become infinite for the column of infinite efficiency simulated by the ideal model. Under the latter conditions, the peak fronts are vertical; the bottom and the top of the peak front of the second component co-elute with the same concentration of the first component; consequently, they are subjected to the same tag-along effect and, when the injection concentration is increased, the front bottom of the second peak is no longer affected by an additional band broadening detrimental to the recovered amount of the first component.

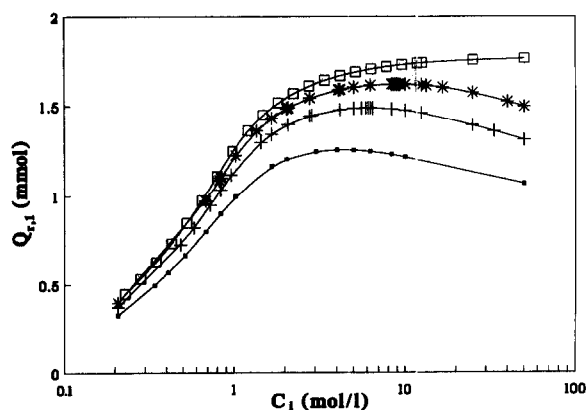


Fig. 13. Plot of the recovered amount of 99% pure solute 1 versus the injected sample concentration for different column efficiencies. Mixture A, relative composition 9:1.  $Q_i = 2.4$  mmol =  $0.4w_s$ . (■)  $n_c = 100$  ( $N_1 = 152$ ;  $N_2 = 135$ ); (+)  $n_c = 200$  ( $N_1 = 302$ ;  $N_2 = 268$ ); (\*)  $n_c = 400$  ( $N_1 = 602$ ;  $N_2 = 535$ ); (□) ideal model ( $N_1$  and  $N_2$  are infinite).

## CONCLUSIONS

The chromatogram of a binary mixture simulated by the Craig model CRAIGSIM is very close to that described by the ideal model. The predictions of CRAIGSIM seem to be quantitative. Hence it was possible to simulate accurately preparative separations and to discuss quantitatively the influence of different parameters such as sample amount, injection volume, injected concentration and column plate number on recovery yield and recovered solute amount at a specified purity.

This work confirms that there are optimum injection conditions corresponding to the maximum recovered amount when the solute of interest is both the first-eluted component and the major portion of the sample [1,3], *i.e.*, when the tag-along effect is strong [4]. In all other instances, the results reported by Knox and Pyper [10] seem to be confirmed: for a given sample load, band broadening can be considered to be a minimum and independent of the injection volume up to a critical value of this volume; this explains why the recovered amount at a given purity and yield is maximum and approximately constant as long as the sample concentration exceeds a certain value.

Another conclusion from this study is that solute-solute interactions and chromatographic dispersion are not independent phenomena and that the optimum value of the injection parameters is affected by the column efficiency. In practice, the optimum injection volume can be considered to be directly proportional to the standard deviation of the peak at infinite dilution. The optimum injection concentration is increased with increasing column plate number.

Consequently, in scaling up a separation, two approaches are possible:

(i) When the plate number is different for the two columns, optimization requires three steps: first, the optimum injection volume for the analytical column is experimentally determined; second, the optimum injection volume for the preparative column is calculated from that of the analytical column and the standard deviation of the peak at infinite dilution for the two columns; third, the injectable load is directly adjusted on the preparative column by injecting optimum volumes of successively more concentrated solutions until the preparative specifications of purity and yield are reached.

(ii) When the two columns have the same efficiency, the optimum injection concentration is identical for the two columns. Hence both injection parameters, volume and concentration, are optimized on the analytical column; the optimum injection volume is calculated as described in (i).

## SYMBOLS

$a_j$	origin slope of Langmuir isotherm ( $j = 1$ or $2$ )
$b_j$	coefficient of non-linearity in Langmuir isotherm equation ( $j = 1$ or $2$ ) (l/mol)
$C_i$	injected sample concentration (mol/l)
$C_{j,n,t}^m$	concentration of solute $j$ ( $j = 1$ or $2$ ) in the mobile phase part of stage $n$ at transfer $t$ (mol/l)
$C_{j,n,t}^s$	concentration of solute $j$ ( $j = 1$ or $2$ ) in the stationary phase part of stage $n$ at transfer $t$ (mol/l)
$F_j$	parameter defined by eqns. A3 and A4 for $j = 1$ and $2$ , respectively
$k'_j$	capacity factor of solute $j$ at infinite dilution ( $j = 1$ or $2$ )
$l_k$	element of a converging sequence defined in Appendix (mol/l)
$m_k$	element of a converging sequence defined in Appendix (mol/l)
$n_c$	number of stages in the Craig machine algorithm
$N_j$	number of theoretical plates calculated on solute $j$ at infinite dilution ( $j = 1$ or $2$ )
$p_k$	element of a converging sequence defined in Appendix (mol/l)
$q_k$	element of a converging sequence defined in Appendix (mol/l)
$Q_i$	injected sample amount (mmol)
$Q_{i,j}$	injected amount of solute $j$ ( $j = 1$ or $2$ ), (mmol)
$Q_{j,n,t}$	amount of solute $j$ ( $j = 1$ or $2$ ) in stage $n$ at transfer $t$ (mmol)
$Q_{r,j}$	recovered amount of solute $j$ ( $j = 1$ or $2$ ) (mmol)
$r_j$	recovery yield of solute $j$ ( $j = 1$ or $2$ )
$V_c$	volume of the empty column (ml)
$V_i$	injected volume (ml)
$V_m$	column dead volume (ml)
$w_s$	saturation capacity of the column (mmol)
$\varepsilon$	column total porosity
$\sigma_1$	standard deviation of the Gaussian peak of solute 1 at infinite dilution (ml)

## ACKNOWLEDGEMENT

This work was supported by CEDI SA (Compagnie Européenne d'Instrumentation, Lannemezan, France) within the context of a "CIFRE convention" (No. 0570/88).

## APPENDIX

*Calculation of concentration of solute 1 and 2 in both phases of a stage*

From eqns. 2a, 2b, 4a and 4b, we can write

$$C_{1,n,t}^m = \frac{b_2\varepsilon(C_{2,n,t}^m)^2 + [(1-\varepsilon)a_2 + \varepsilon - b_2F_2]C_{2,n,t}^m - F_2}{b_1(F_2 - \varepsilon C_{2,n,t}^m)} \quad (A1)$$

$$C_{2,n,t}^m = \frac{b_1\varepsilon(C_{1,n,t}^m)^2 + [(1-\varepsilon)a_1 + \varepsilon - b_1F_1]C_{1,n,t}^m - F_1}{b_2(F_1 - \varepsilon C_{1,n,t}^m)} \quad (A2)$$

with

$$F_1 = \frac{Q_{1,n,t}n_c}{V_c} \quad (A3)$$

$$F_2 = \frac{Q_{2,n,t}n_c}{V_c} \quad (A4)$$

Considering eqns. 2a and A3, the following inequalities can be written:

$$0 \leq C_{1,n,t}^m \leq \frac{F_1}{\varepsilon} \quad (A5)$$

$C_{1,n,t}^m$  is equal to 0 and  $F_1/\varepsilon$  when solute 1 is totally retained and non-retained, respectively.

Then, from eqns. A1 and A5, we obtain

$$0 \leq \frac{b_2\varepsilon(C_{2,n,t}^m)^2 + [(1-\varepsilon)a_2 + \varepsilon - b_2F_2]C_{2,n,t}^m - F_2}{b_1(F_2 - \varepsilon C_{2,n,t}^m)} \leq \frac{F_1}{\varepsilon} \quad (A6)$$

from which it can be demonstrated that

$$l_1 \leq C_{2,n,t}^m \leq m_1 \quad (A7)$$

with  $0 \leq l_1 \leq m_1 \leq F_2/\varepsilon$ . Substitution of eqn. A2 in eqn. A7 leads to

$$p_1 \leq C_{1,n,t}^m \leq q_1 \quad (A8)$$

with  $0 \leq p_1 \leq q_1 \leq F_1/\varepsilon$ . The calculation is then

iterated: substitution of eqn. A1 in eqn. A8 leads to

$$l_2 \leq C_{2,n,t}^m \leq m_2 \quad (\text{A9})$$

with  $0 \leq l_1 \leq l_2 \leq m_2 \leq m_1 \leq F_2/\varepsilon$ , and substitution of eqn. A2 in eqn. A9 leads to

$$p_2 \leq C_{1,n,t}^m \leq q_2 \quad (\text{A10})$$

with  $0 \leq p_1 \leq p_2 \leq q_2 \leq q_1 \leq F_1/\varepsilon$ , and so on.

At the  $k$ th iteration  $l_k \leq C_{2,n,t}^m \leq m_k$  and  $p_k \leq C_{1,n,t}^m \leq q_k$ , where the sequences  $l_k$  and  $m_k$  and the sequences  $p_k$  and  $q_k$  converge to  $C_{2,n,t}^m$  and  $C_{1,n,t}^m$ , respectively.  $m_k$  and  $q_k$  are considered to be equal to  $C_{2,n,t}^m$  and  $C_{1,n,t}^m$ , respectively, when  $(m_k - l_k)/l_k \leq \lim$  and  $(q_k - p_k)/p_k \leq \lim$ ,  $\lim$  being fixed *a priori*.  $C_{1,n,t}^s$  and  $C_{2,n,t}^s$  are then calculated from eqns. 4a and 4b.

## REFERENCES

- 1 G. Crétier and J. L. Rocca, *Sep. Sci. Technol.*, 22 (1987) 1881.
- 2 A. Katti and G. Guiochon, *Anal. Chem.*, 61 (1989) 982.
- 3 V. Svoboda, *J. Chromatogr.*, 464 (1989) 1.
- 4 J. Newburger and G. Guiochon, *J. Chromatogr.*, 484 (1989) 153.
- 5 G. Guiochon and S. Ghodbane, *J. Phys. Chem.*, 92 (1988) 3682.
- 6 B. L. Karger, L. R. Snyder and Cs. Horváth, *An Introduction to Separation Science*, Wiley-Interscience, New York, 1973, p. 110.
- 7 L. R. Snyder, J. W. Dolan and G. B. Cox, *J. Chromatogr.*, 483 (1989) 63.
- 8 S. Golshan-Shirazi and G. Guiochon, *J. Phys. Chem.*, 93 (1989) 4143.
- 9 R. M. Nicoud and H. Colin, *LC GC Int.*, 3, No. 2 (1990) 28.
- 10 J. H. Knox and H. M. Pyper, *J. Chromatogr.*, 363 (1986) 1.